Macromolecular Bioscience
www.mbs-journal.de

A Humanized In Vitro Model of Innervated Skin for Transdermal Analgesic Testing

*Afonso Malheiro, Maria Thon, Ana Filipa Lourenço, Adrián Seijas Gamardo, Amit Chandrakar, Susan Gibbs, Paul Wieringa, and Lorenzo Moroni**

Sensory innervation of the skin is essential for its function, homeostasis, and wound healing mechanisms. Thus, to adequately model the cellular microenvironment and function of native skin, in vitro human skin equivalents (hSE) containing a sensory neuron population began to be researched. In this work, a fully human 3D platform of hSE innervated by induced pluripotent stem cell-derived nociceptor neurospheres (hNNs), mimicking the native mode of innervation, is established. Both the hSE and nociceptor population exhibit morphological and phenotypical characteristics resembling their native counterparts, such as epidermal and dermal layer formation and nociceptor marker exhibition, respectively. In the co-culture platform, neurites develop from the hNNs and navigate in 3D to innervate the hSE from a distance. To probe both skin and nociceptor functionality, a clinically available capsaicin patch (Qutenza) is applied directly over the hSE section and neuron reaction is analyzed. Application of the patch causes an exposure time-dependent neurite regression and degeneration. In platforms absent of hSE, axonal degeneration is further increased, highlighting the role of the skin construct as a barrier. In sum, an in vitro tool of functional innervated skin with high interest for preclinical research is established.

1. Introduction

The skin is densely innervated by different sensory nerve fibers that equip individuals with the ability to sense touch, temperature, and pain.[1,2] This permits the recognition and avoidance of damaging stimuli, which is pivotal to maintain the physical integrity of skin (and other organs).[3] For this, cutaneous nociceptor fibers play a major role, by detecting noxious stimuli, such as high temperature (>43 °C), low pH substances (<6.0), and irritant chemicals (e.g., capsaicin), and conveying a signal to the central nervous system (CNS).[4] Noxious stimuli detection is provided by sensor proteins, such as transient receptor potential vanilloid 1 (TRPV-1) channels, expressed within nociceptor fibers. Once activated, these channels open and induce neuron depolarization, triggering an action potential that is further propagated to the CNS, where a pain is perceived.[4,5] Interestingly, the continuous targeting of TRPV-1 channels with a stable agonist, such as capsaicin, can induce nociceptor desensitization and nerve ending ablation, which results in a local analgesic effect instead.[4] In addition to providing sensorial ability, skin innervation is also necessary to maintain skin physiology and to promote re-epithelialization during wound healing.[2,6,7,8] Thus, cutaneous nerves are not only essential for normal skin function, but also for restoring function after damage. Moreover, nerve defects due to pathological conditions, such as spinal cord injury or diabetic neuropathy, lead to impaired regeneration.[1]

In recent years, the development of engineered human skin equivalents (hSE) has greatly evolved and several companies are now commercializing skin analogues composed of fibroblasts and keratinocytes that replicate the skin anatomy up to an extent.[3] Such models constitute a safe, inexpensive, and quick alternative to animal testing and simultaneously provide a more translational research tool, due to their human source. Because of their defined cellular ecosystem, in vitro models also permit a simpler and more direct evaluation of specific cells and molecules contribution. Advanced hSE models containing other cellular components such as vasculature,[9] hair follicles,[10] and melanocytes[11] have been developed in order to better mimic the native microenvironment, to study specific interactions and to accurately model certain pathologies. Despite these

A. Malheiro, A. F. Lourenço, A. S. Gamardo, A. Chandrakar, P. Wieringa, L. Moroni
MERLN Institute for Technology-Inspired Regenerative Medicine
Complex Tissue Regeneration Department
Maastricht University
Universiteitssingel 40, Maastricht 6229ER, The Netherlands
E-mail: l.moroni@maastrichtuniversity.nl

M. Thon, S. Gibbs
Department of Molecular Cell Biology and Immunology
Amsterdam University Medical Centre
Amsterdam Infection and Immunity Institute
Vrije Universiteit Amsterdam
Amsterdam 1081HV, The Netherlands

S. Gibbs
Department of Oral Cell Biology
Academic Centre for Dentistry (ACTA)
University of Amsterdam and Vrije Universiteit Amsterdam
Amsterdam 1182DB, The Netherlands

The ORCID identification number(s) for the author(s) of this article can be found under https://doi.org/10.1002/mabi.202200387

DOI: 10.1002/mabi.202200387

advancements, innervated hSE platforms are still scarce, regardless of the importance of cutaneous nerves for skin function and wound regeneration mechanisms. The development of innervated hSE models would improve in vitro testing by providing more representative data and allowing a wider range of assays that probe neurons state and their influence on surrounding cells. This is of particular interest to screen compounds with potential neurotoxic effects and/or that may produce/mitigate pain,[12] to design strategies for improved wound healing via nerve targeting[7] or to investigate nerve relations with other cell types in health and pathological states (e.g., diabetic neuropathy).[3] To show the influence of nerves on skin regeneration, Blais et al.[6] constructed a skin model containing mouse sensory neurons, which upon implantation on a wounded mouse, led to faster wound regeneration (due to substance P secretion) compared to control constructs (absent of neurons). However, due to the physiological differences between species, research using innervated skin models fully composed of human cells is needed. To this end, Muller et al.[13] reported an innervated hSE model containing functional nociceptors obtained from induced pluripotent stem cells (iPSCs). Despite the successful integration of all cellular components, the reported strategy still presented some shortcomings such as disorganized and non-representative neuronal architecture, with neural cell bodies situated beneath the skin tissue; because of this configuration, sample sectioning is required to observe innervation pattern. Moreover, testing on this model remains to be demonstrated.

In this work, we show the development of an innervated hSE model with demonstrated applicability. The model is comprised of a fibrin/collagen hydrogel platform containing two separate compartments, one for a sensory neuron population and the other for a hSE construct. Sensory neurons were differentiated from iPSCs as previously described,[14] formed into a neurosphere, and exposed to nerve growth factor (NGF) to induce a mature nociceptor phenotype (TRPV-1$^+$ and response to noxious stimuli) as well as electrical activity. The fabrication method of the hSE was also previously reported and the engineered tissue well-characterized.[15,16] In this co-culture system, the neurospheres were able to develop extensive neurite projections throughout the gel platform, to innervate the hSE from a distance within 21 days. Co-cultures with primary neurons from a dorsal root ganglion (DRG) population instead, revealed similar neuron morphologies although innervating at a higher density. To validate the platform utility, we performed a topical application of a commercial capsaicin patch (Qutenza) on the skin region and detected a time-dependent neural degradation of nociceptors neurospheres (hNN) and DRG neurons as a result. In sum, the work here described constitutes an advancement in the development of fully human and functional innervated hSE constructs that permit convenient testing and tissue analysis.

2. Results

2.1. Fabrication of a Human Nociceptor 3D Culture Model

To generate functional human nociceptor spheroids (hNNs), we followed a previously reported protocol,[14] which is illustrated in **Figure 1**A. At day 9 of differentiation, the mold contains a large collection of uniform, cohesive, and round spheroids with an average diameter of 308.7 ± 38.6 μm (Figure 1B). At this stage, the spheroids are harvested from the mold, transferred to the culture substrate and cultured for at least 7 days in NGF-supplemented neural medium to promote neurite outgrowth and nociceptor phenotype acquisition in situ. When cultured on laminin-coated (1 μg mL^{-1}) coverslips, the neurons were able to attach, survive and grow neurites. We showed neurite outgrowth from an hNN cultured for 7 days in neural medium (Figure 1C), evidencing a dense and radial neurite projection (βIII-tubulin$^+$ segments). To validate the acquisition of a nociceptor phenotype, we investigated the presence of characteristic nociceptor markers,[17] TRPV-1, calcitonin gene-related peptide (CGRP), and substance P, and compared it with primary sensory neurons, obtained from a rat DRG explant (Figure 1D). Both hNN neurons (Figure 1D, top row) and DRG neurons (Figure 1D, bottom row) revealed the presence of these markers, located throughout the axonal length.

After phenotypical evaluation, we developed and analyzed a 3D culture model for hNN, using DRG cultures as a comparison. The model is composed of a 12-mm polyurethane scaffold supporting the hNN or DRG, which are cultured in neural medium. After overnight attachment, the cell-seeded scaffold was covered with a solution of collagen/fibrin (at 4 and 1 mg mL^{-1}, respectively), that quickly gelled and formed a stable hydrogel. In 7 days old models, both cell types could develop dense and extensive neurite projections throughout the gel (Figure 1E). After this culture period, the neurite length for hNNs and DRGs was not significantly different and exhibited a mean value of 488.6 and 503.5 μm, respectively (Figure 1F).

2.2. Development of a Human Skin Equivalent

To generate a human skin equivalent (hSE) we used a protocol previously established[16] and illustrated in **Figure 2**A. After this culture period, the hSE construct appeared as a compact, opaque, elastic, and circular tissue with an area of 159 ± 7 mm^2 and approximate diameter of 14 mm (Figure 2B). During formation, the surface area reduced by ≈20%–30% of the original size due to fibroblast presence. Although direct measurement of the hSE mechanical properties was not possible due to technical limitations, we estimate the stiffness of our skin equivalent is between 54 Pa (Figure S10, Supporting Information, acellular collagen/fibrin hydrogel) and 360 Pa, the reported stiffness of native skin.[18] To analyze skin maturation, we performed histological and immunohistochemical analysis on the cross sections (Figure 2C,D). As visible from H&E staining (Figure 2C), the engineered tissue remarkably resembled the native skin structure[19] evidencing the formation of a dermis (hydrogel region with dispersed fibroblasts) and epidermis region (compact stratified cell layer culminating in a stratum corneum). Particularly, the hSE was characterized by the dermal–epidermal transition zone where cuboidal keratinocytes could be observed at the epidermis bottom, which then transition to slightly elongated keratinocytes until the top epidermal part where the keratinocytes are very elongated. In addition, the presence of suprabasal keratin 10 (Figure 2D left; in red) and stratum granulosum loricrin (Figure 2D right; in red) in the epidermal region of the hSE construct was detected.

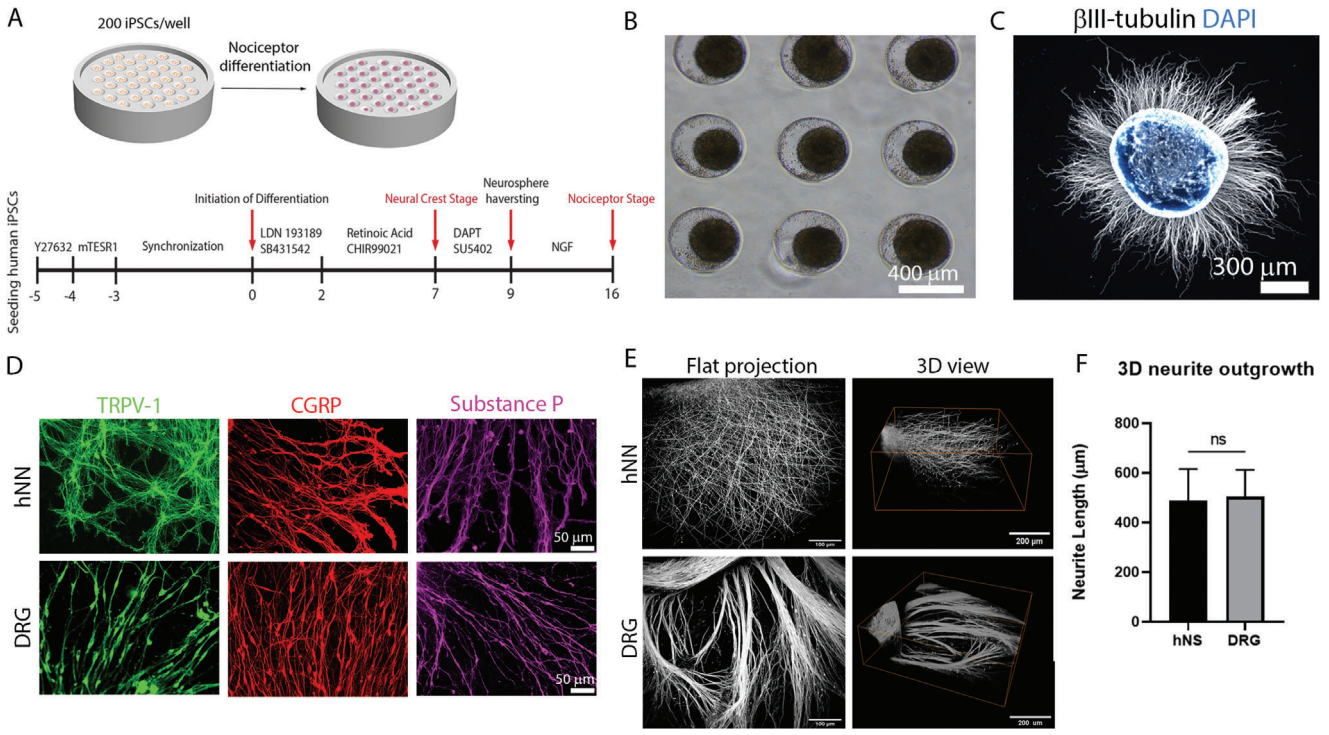

Figure 1. Development and characterization of iPSCs-derived nociceptors and 3D culture within fibrin/collagen hydrogels. A) Illustration of the process for iPSCs differentiation into nociceptors and spheroid formation. B) Brightfield microscopy image of the agarose mold showing the formation of spherical, compact, and uniform neuron clusters with an average diameter of 308.7 ± 38.6 µm. Scale bar is 400 µm. C) Neurite outgrowth from the hNN after 7 days of culture on a laminin-coated coverslip. βIII-tubulin is shown in white and DAPI in blue. Scale bar is 300 µm. D) Characterization of the nociceptor phenotype from iPSCs-derived nociceptors (top row) and comparison with rat DRG neurons (bottom row). Both cell types were cultured for 7 days on laminin-coated coverslips and both show the expression of the characteristic nociceptor markers: TRPV-1 (green, left column), CGRP (red, middle column), and substance P (purple, right column). Scale bar is 50 µm for all images. E) 3D culture of hNNs (top row) and rat DRGs (bottom row) on a collagen/fibrin hydrogel for 7 days, demonstrating extensive neurite outgrowth throughout the gel, as visible through the flat projection (left column, scale bar is 100 µm) and 3D view (right column, scale bar is 200 µm). Representative images of three independent experiments are shown. F) Neurite outgrowth from human nociceptor spheroids (hNN) (black bar) or rat DRGs (gray bar) in collagen/fibrin hydrogels. The bar graph represents the mean ± SD obtained from neurite length measurements in images containing the full neurite length. At least ten measurements were taken per image and three images were taken per sample ($n = 4$). Statistics were performed with an unpaired t-test and ns denotes $p > 0.05$.

2.3. Development of a Skin Innervation Model in Compartmentalized Hydrogel Platform

In order to fabricate a skin innervation model that is reproducible, biomimetic and permits a facile morphological assessment of both tissues, we developed a compartmentalized hydrogel platform. For this, we used custom made polydimethylsiloxane (PDMS) molds (Figure S1, Supporting Information) to pattern two separate compartments within a collagen/fibrin hydrogel with 1.5 mm in height, measuring 1 and 3 mm in diameter, and intended for a neural population (hNN or DRG) and hSE section, respectively. The distance between compartments was purposely set at 1 mm, in order to have sufficient mechanical stability at the separating hydrogel layer and to better observe remote innervation. To fabricate the platform, we followed the process illustrated in **Figure 3**A. A mesh support of nonwoven polyurethane was used to provide stable anchorage points to the hydrogel, facilitating the removal from the mold and future handling. After overnight polymerization, the patterned gels could be easily removed and maintained their structural stability, evidencing the presence of two separate compartments, separated by 1 mm (Figure 3B,C; a red dye was added to improve contrast).

For the preparation of the skin innervation model we followed the timeline illustrated in Figure 3D, using either one hNN or DRG as neuron population. After implantation of the hSE section on the skin compartment, the platform was lifted to air and cultured for 21 days, with both tissues segregated but in proximity (Figure 3E). Following 21 days of co-culture, we evaluated the neuronal outgrowth and the occurrence of innervation. hNNs developed a dense and radial neurite network with long neurite projections (marked by βIII-tubulin) averaging 1786.6 µm in length (**Figure 4**A). Examining the border of the hSE section (marked by involucrin) at high magnification, it was possible to observe the occurrence of innervation, denoted by the presence of several neurites that grew into the skin region (Figure 4B,C). In DRG-containing platforms, we registered a similar neurite outgrowth pattern after the same culture period (Figure S2A, Supporting Information). The mean neurite length was 2546.3 µm and extensive innervation was also detected (Figure S2B, Supporting Information). In both systems, the hSE and surrounding matrix did not further contract, despite potential

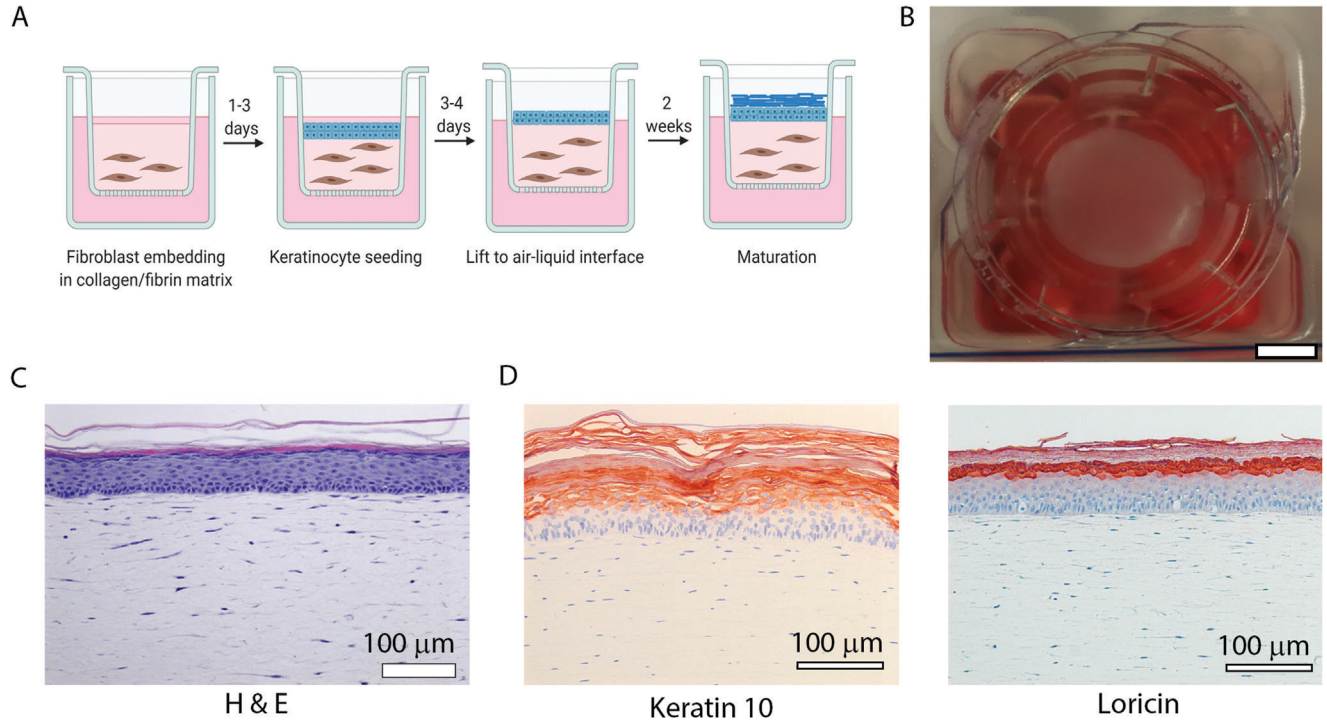

Figure 2. Development of a human skin equivalent composed of human keratinocytes and human fibroblasts in a collagen/fibrin matrix. A) Illustration of the followed protocol. In the first stage, fibroblasts are embedded in a collagen/fibrin matrix at a density of 5×10^5 cells/hydrogel (in 350 µL) and cultured in submerged conditions for 1–3 days. Keratinocytes (5×10^5 cells) are then seeded on top of the gel and cultured in submerged conditions for 3–4 days. After this, the construct is lifted to an air–liquid interface to induce epidermal differentiation. The constructs are cultured for additional two weeks for further skin maturation. B) Photograph of the skin construct at the end stage of the protocol. Scale bar is 5 mm. C) Hematoxylin and eosin (H&E) staining on a skin equivalent cross section showing the formation of dermis and epidermis, containing all characteristic layers. Scale bar is 100 µm. D) Expression of keratin 10 (red, left image) and loricrin (red, right image) on skin equivalent layers. Samples were counterstained with hematoxylin (blue). Scale bar is 100 µm. Illustration was made in biorender (https://biorender.com/).

skin fibroblast proliferation and invasion of the surroundings. We believe that the underlying nonwoven scaffold acted as a stabilizer and prevent platform contraction.

To quantify the innervation area in models composed of hNNs or DRGs, we acquired images of neurites present at the border of the hSE construct and penetrating into it. iPSCs-derived cells were able to generate a large innervation area (6.8×10^5 pixel area mm^{-2}), with DRGs producing an even higher number ($p < 0.05$) of innervating axons (1.7×10^6 pixel area mm^{-2}) (Figure S3, Supporting Information).

2.4. Innervated Skin Model Function Testing by Capsaicin Patch Application

After characterization of a platform showing nociceptor innervation of a hSE construct, we performed an experiment that allowed simultaneous testing of the hSE and nociceptor function. For this, we applied a capsaicin patch topically (directly over the hSE section) for 1 or 24 h and measured the neural response (**Figure 5**A). As a control we used samples that were not exposed to the capsaicin patch. To investigate the influence of the skin barrier, we also tested platforms composed of hNN but lacking the hSE component. In these samples, the capsaicin patch was placed inside the void skin compartment. For comparison, we also realized this experiment on platforms composed of primary nociceptors from a rat DRG population (Figure S5, Supporting Information).

The capsaicin patch was absorbed through the skin and delivered to the innervating neurites, causing subsequent degeneration. These morphological changes were evident when comparing to control samples, in which normal neurite morphology was observed with no signs of injury (Figure 5Bi). On the other hand, after 1 h of exposure (Figure 5Bii), neural degeneration (ND) was visible through the formation of blebs throughout the axonal network. If exposure to capsaicin was prolonged to 24 h, axonal degeneration was even more pronounced (Figure 5Biii). At this time point, bleb formation (BF) was ubiquitous and a loss of neurite alignment was observed (BF was 1318.0 ± 226.9). The appearance of blebs was significantly increased compared to control samples ($p < 0.001$; BF was 343.0 ± 110.3) and 1 h treated samples ($p < 0.05$; BF was 805.8 ± 464.9) (Figure 5C). Axonal degeneration measurements also revealed significantly more degraded neurites in 24 h-treated samples (ND was 0.04 ± 0.009) compared to those treated for 1 h ($p < 0.01$; ND was 0.021 ± 0.015) and control samples ($p < 0.001$; ND was 0.007 ± 0.002). In addition to degradation, we also observed signs of neurite retraction (pointed by white arrows in Figure 5Biii). We investigated neurite retraction in 2D hNN cultures (on laminin-coated coverslip) and saw that 24 h of capsaicin exposure (at 100×10^{-6} M) routinely formed wave fronts, resultant of pulled-back

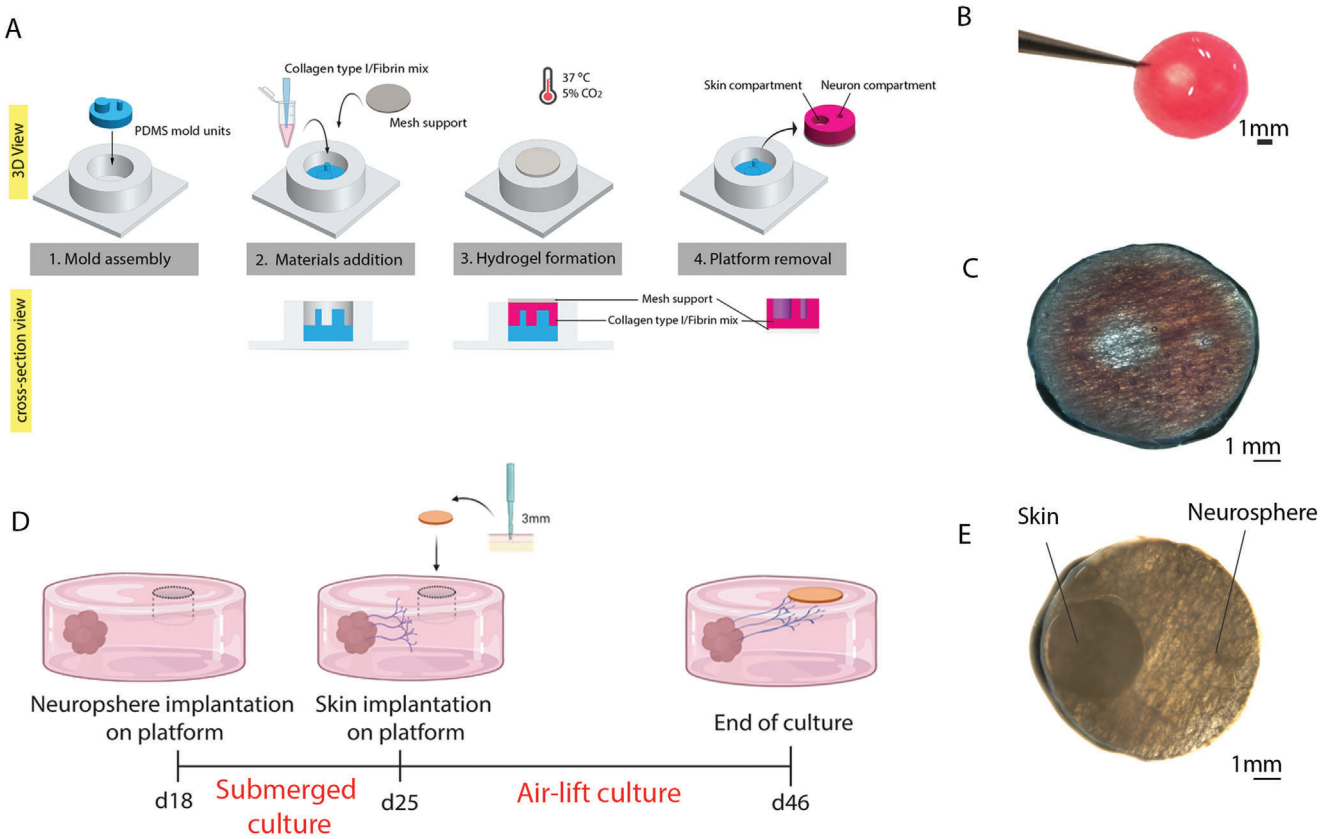

Figure 3. Fabrication of a collagen/fibrin platform with defined compartments for hSE and hNN. A) Illustration of the fabrication process. First, the PDMS mold units are assembled as demonstrated, with the pillars of the patterning unit facing up. Then, 150 µL of a chilled collagen/fibrin mix solution is pipetted into the mold and a mesh support is placed on top. The gel is left to form overnight in the incubator at 37 °C, 5% CO_2. The day after, the gel can be removed. B) Photograph of a gel evidencing the two wells for cell culture. The red color is from a red dye, added to improve visualization. Scale bar is 1 mm. C) Stereomicroscope micrograph showing in better detail the presence of compartments, for skin placement (3 mm; left compartment) and for neuron population seeding (1 mm; right compartment). D) Depiction of the followed protocol for the formation of an innervated skin platform. The timeline is relative to the beginning of the iPSCs culture protocol shown in Figure 1. Initially the hNN is implanted on the platform within the neural compartment. After 7 days of culture in submerged conditions with neural medium, the hSE section is added. For this, we take a 3 mm biopsy from a larger hSE construct and carefully add it to the platform. A 10 µL collagen/fibrin drop is added to bond it to the platform. The platforms are lifted to an air–liquid interface and cultured for 21 days with neural/skin medium at 1:1. E) Stereomicroscope micrograph showing the presence of a hSE section and a neurosphere in their defined compartments. Scale bar is 1 mm. Illustration in (D) was made in biorender (https://biorender.com/).

neurites (Figure S4, Supporting Information). Moreover, we also saw that 24 h exposure could lead to the detachment of neural tissue in some areas (Figure S5B, Supporting Information). Contrarily, control samples (Figure S5A, Supporting Information) exhibited good neural tissue stability throughout the hydrogel. Innervation platforms composed of DRGs neurons showed a similar response as in hNN-containing platforms (Figure S7, Supporting Information), with the capsaicin treatment leading to a time-dependent axonal degeneration with identical morphological changes. After 1 h of incubation degradation was still low (Figure S8, Supporting Information; BC was 993.2 ± 402.4; ND was 0.039 ± 0.020), but after 24 h the neurites morphology exhibited clear signs of damage (Figure S8, Supporting Information; BC was 2252.0 ± 507.3; ND was 0.1314 ± 0.04277) at a larger extent than hNN samples. In samples lacking a skin construct (Figure 5B bottom row), we could see that capsaicin diffusion was unhindered and thus neurite degeneration was even more pronounced. After 1 h of exposure (Figure 5B v), a vast neurite degeneration and retraction was already observed (Figure S9, Supporting Information; BC was 1929 ± 198.3; ND was 0.087 ± 0.042). Axonal degeneration was further increased when the exposure time was 24 h (Figure 5B vi), as most of the neurite network was destroyed or severely damaged (Figure S9, Supporting Information; BC was 2610 ± 1815; ND was 0.15 ± 0.10).

3. Discussion

Cutaneous sensory innervation is necessary to provide skin with its sensorial function and to promote efficient wound healing.[1,8] Therefore, their presence within hSE is critical to better recapitulate the native skin structure/function, as well as to investigate pathologies involving cutaneous nerve fibers (e.g., diabetes)[20] and wound healing mechanisms/acceleration strategies.[6,21] In particular, nociceptor fibers are essential to prevent organ damage, by mediating the pain sensing mechanisms that recognize noxious stimuli in direct (e.g., capsaicin) or indirect (e.g., high temperature) contact with the skin. Through this sensation ability, avoidance of insults is triggered and tissue integrity can be

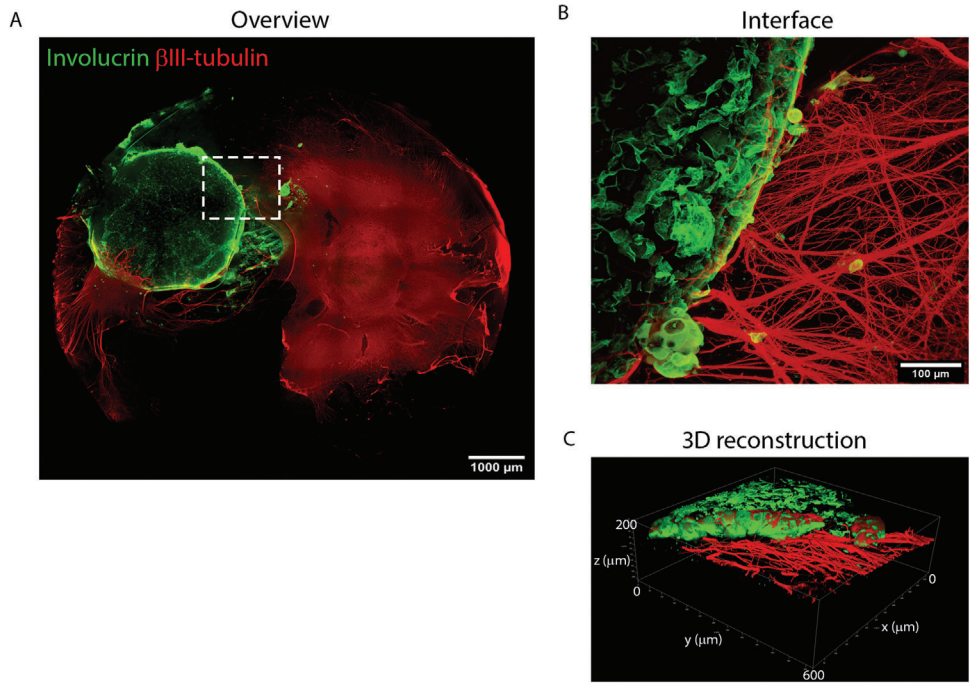

Figure 4. Remote innervation of a hSE section within the compartmentalized collagen/fibrin platform. A) Overview of the platform showing a vast neurite outgrowth (βIII-tubulin, red) from the hNN toward the hSE compartment (involucrin, green). Scale bar is 1000 µm. B) High-magnification view of the white dashed rectangle marked in (A). In the interface between the hSE section and the surrounding gel a large amount of neurites that penetrate into the hSE compartment are visible. Scale bar is 100 µm. C) 3D reconstruction of the interface view shown in (B). Representative images of one experiment ($n = 4$) are shown.

maintained.[1,17,22] Thus, in vitro hSE models incorporating nociceptors will also open the possibility to investigate the influence of compounds on skin and the underlying nerves (e.g., cosmetic, therapeutic creams, etc.),[12] which is of utmost interest to several research and industrial applications.

The goal of this work was to develop a 3D biomimetic model of human skin with innervating nociceptors. At the same time, we intended to design a platform that simplified in vitro testing, such as morphological evaluation of the innervating fibers. To achieve this, we fabricated a hydrogel platform containing two separate wells, for compartmentalized co-culture of a nociceptor population (hNN) and a skin equivalent (hSE) (Figure 3). The compartmentalization of tissues ensures reproducible and precise cell location, consistent nerve fiber length/innervation density and replicates the native mode of cutaneous innervation from a distant DRG.[23] In addition, assessment of the innervating fibers can be done directly in whole-mount samples, thus avoiding the laborious and time-consuming process of sample sectioning. As a hydrogel material, we used a collagen/fibrin blend, which permits the simple and quick preparation of a patterned hydrogel with a stable shape. Moreover, these materials are permissive for both neural and skin cells growth and have been extensively used in skin and nerve tissue engineering approaches.[24,25] hNN were obtained as previously described,[14] using a method that yields a large number of self-aggregating and uniformly sized cell clusters (Figure 1A,B), which not only simplifies the tissue production process, but also ensures reproducibility between samples. Cultured hNN promptly outgrow neurites in 2D (Figure 1C) and 3D (Figure 1E), and express several nociceptors markers (Figure 1D) that indicate their functionality as pain-sensing neurons. Contrary to other reports of iPSCs-derived nociceptors,[13] the neurons here formed are bundled in a cluster that mimics the native morphology of a DRG and preserves neuron–neuron interactions at the soma.[14] Furthermore, by maintaining the neurons within the cluster, neurites project outwards, which not only approximates the native mode of innervation, but also simplifies quantification analysis. 3D neural growth in collagen/fibrin matrices (Figure 1E), demonstrated that our human nerve model can be compared to the animal-DRGs in terms of size. Because of the simplicity and productivity of the process, clinical relevance of the cell model and lack of animal sacrificing, these results highlight the vast superiority of this approach compared to conventional animal-DRG dissection and use.

To fabricate a hSE model we used a well-established and reported method[15,16] that generates a skin-like tissue with remarkable morphological resemblance to the native tissue,[26] with clear formation of a dermis and stratified epidermis region (Figure 2B–D). From a single skin sheet, several punches can be performed to increase sample output and also ensure tissue reproducibility. To assemble the innervated skin model, we added the neural and skin tissues sequentially to the hydrogel platform, starting with the neural cell cluster, in order to prime neurite outgrowth within the hydrogel, before hSE implantation (Figure 3D). Co-cultures of 21 days resulted in a vast and radial 3D neurite outgrowth that reached and innervated the hSE section (Figure 4). It is worth noting that neurite outgrowth happened radially and was not specifically targeted to the hSE. Comparative co-cultures with a primary DRG explant led to a similar neurite density, but with increased

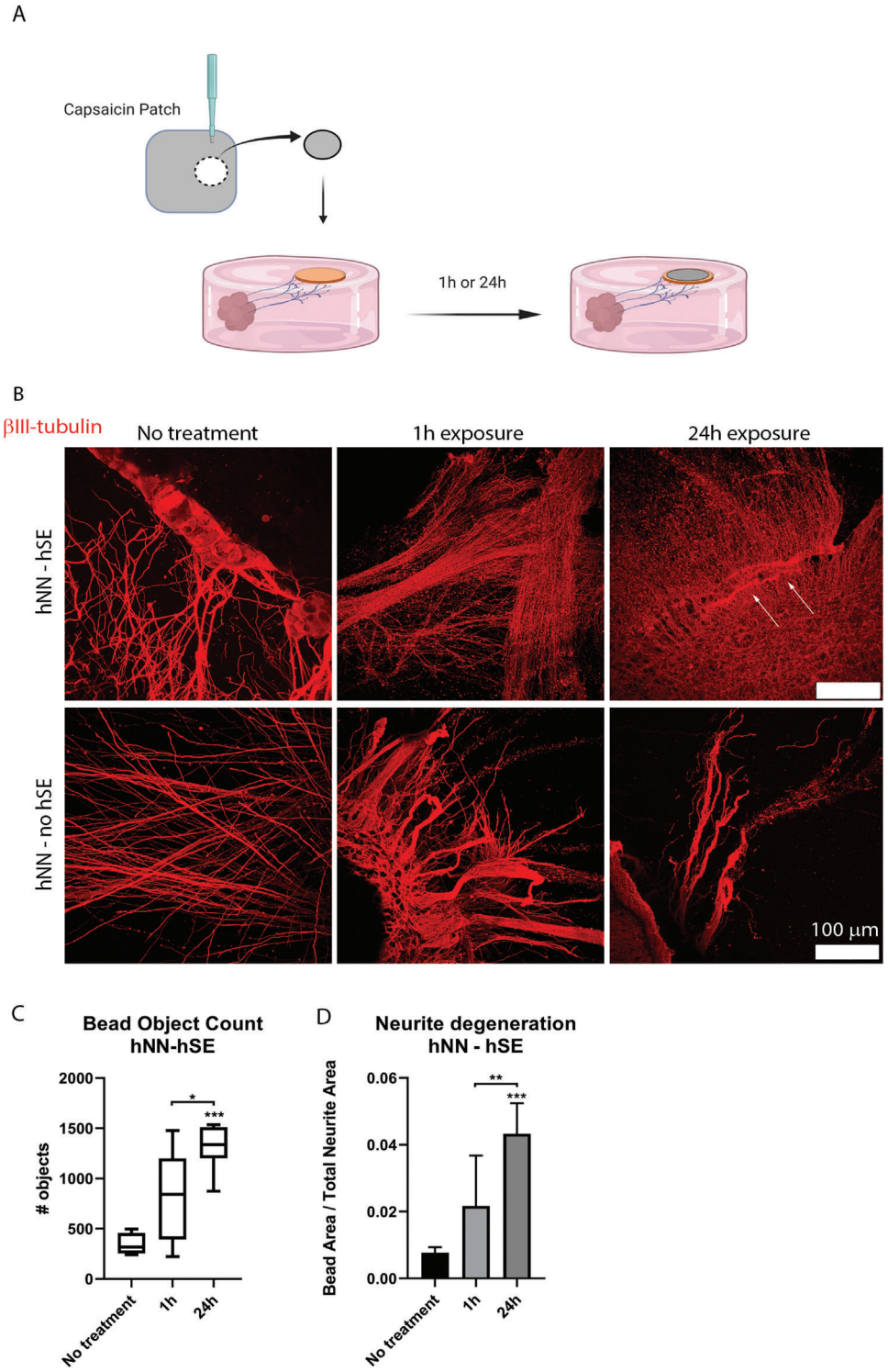

Figure 5. Nociceptor response to a capsaicin stimulus applied via a capsaicin patch, placed over the skin section. A) Illustration of the followed approach. A 3 mm cut of a large capsaicin patch was made with a biopsy punch and carefully placed over the skin. The samples were incubated for 1 and 24 h and then analyzed. Illustration was made in biorender (https://biorender.com/). B) Immunostaining to βIII-tubulin (in red) revealed that a capsaicin stimulus applied on the skin is absorbed and transmitted to the surrounding neurons, causing an exposure time-dependent degradation. After 1 h of exposure (top row, middle column) the signs of neurite degeneration are already evident. After 24 h of exposure (top row, right column) the amount of degenerated neurites increased and there were also signs of neurite retraction. In no treatment samples (top row, left column), the neurite morphology seemed normal, with no signs of injury. Samples with no added hSE (bottom row) showed that in the absence of a skin layer between the capsaicin patch and the gel platform, capsaicin diffusion was enhanced and consequently the effect over hNN at 1 h (middle image) or 24 h (right image) was even more pronounced. All scale bars are 100 µm. C,D) Quantification of the axonal degeneration observed in this experiment within the innervated hSE

targeting toward the hSE that resulted in a larger innervation density compared to hNN-hSE models (Figures S2 and S3, Supporting Information). Here, our objective was not to provide a side-by-side comparison, but rather to demonstrate that our differentiated cells exhibited a similar phenotype and growth/innervating capacity to primary nociceptors, thus validating their applicability.

Once the skin innervation model was established, we devised an experimental setup to simultaneously evaluate the skin barrier function and nociceptor ability to detect noxious stimuli. To do this, we applied a commercially available capsaicin patch (Qutenza) in contact with the hSE and directly measured the nociceptors reaction, via fluorescent imaging of the whole sample (Figure 5A). Despite causing irritation and a burning sensation, capsaicin treatments are used in the clinic as a pain management solution; the molecule is able to selectively target and stimulate nociceptors, causing their reversible defunctionalization/ablation.[4,27] In particular, the Qutenza patch delivers a high capsaicin concentration (80 mg capsaicin per gram of adhesive; 8%) and is shown to produce an effective pain relief for up to 12 weeks, after a single 60 min application.[4] Capsaicin activates TRPV-1 channels, promoting calcium influx and consequent mitochondrial dysfunction, inhibition of metabolism and loss of electrical excitability, leading to loss of function. In addition, the maintenance of cellular membrane integrity may be compromised, resulting in the collapse/retraction of nerve endings.[4,28] In our experiment with hNN-hSE platforms, we observed that the capsaicin treatment led to the appearance of blebs within the neurite network, indicating neurite degeneration, in proportion to the patch application time (Figure 5B–D). This was evident when compared to the control samples, whose neurite networks appeared straight and with no beads. Because of these obvious morphological changes, we could quantify neurite degeneration, with an in-house developed imaging algorithm that tracked bead formation (Figure S6, Supporting Information). We also observed neurite retraction as a consequence of capsaicin treatment in our 3D platform (Figure 5B) and in 2D cultures (Figure S4, Supporting Information), indicating a similar behavior of these differentiated nociceptors compared to their native counterparts.

In the absence of a hSE construct, neurite damage was even more pronounced, exhibiting extensive degeneration already after 1 h of patch exposure and almost full neurite ablation after a 24 h treatment (Figure 5B bottom row and Figure S10, Supporting Information). This finding underscores the ability of our skin construct to act as a barrier that slows the delivery of capsaicin to innervating fibers. In DRG containing platforms we also detected the same neurite regression and degeneration effect after capsaicin exposure (Figure S7, Supporting Information), which indicates that our differentiated neurons replicate the primary neuron response to noxious stimuli. However, the neurite damage was further accentuated in DRGs, compared to differentiated nociceptors (Figure 5C,D and Figure S8, Supporting Information), probably due to a higher expression of TRPV-1 and thus increased sensitivity to capsaicin.

As demonstrated, this platform can support testing of compounds with potential effects on cutaneous nerves, applied via a method that mimics real topical applications. Particularly, substances that activate nociceptors and may trigger a painful sensation, as well as cause neurotoxicity, could be evaluated with this platform. Due to our platform design denoted by two horizontally separate compartments, testing is simplified by the ability to directly observe the innervating fibers without need for sample sectioning. This is an improvement from other hSE models[13] where the stacked configuration of neurons and skin tissue requires sectioning to observe innervating fibers.

Despite showing a platform with well-established and reproducible tissue-engineered models of both nerves and skin, the present work still contains some limitations. Particularly, the soft nature of the hydrogel blend composing the platform is prone to irregularities which can affect sample reproducibility. Performing these experiments is also a challenging aspect, since the overall culture period is 46 d, which requires a large investment of time and resources (e.g., culture medium). However, when comparing to animal breeding, experimentation and sacrificing, this protocol is vastly more economical and time efficient.

Our previous work[14] demonstrated that iPSC-derived neurons could be stimulated to release CGRP and substance P (neuropeptides involved in nociceptive pain) after TRPV-1 stimulation with a capsaicin analog. Further quantification of neuropeptide release (e.g., via ELISA) would strengthen the experimental read-out, allowing to better determine the response of our model to noxious stimuli. In addition, testing of noxious stimuli of different nature, such as mechanical (e.g., pinching) or thermal (e.g., high temperature), would further characterize this model and shed light on the versatility of applications. The acquisition of histological and immunohistochemical cross-sectional images of the model after the co-culture period (and capsaicin exposure) would permit the evaluation of hSE quality, as well as epidermal nerve fiber density/morphology. Future work should also aim at incorporating Schwann cells to assess the role of myelinated fibers in skin innervation, as well as the improvement of skin function as a consequence of innervating fiber presence, for instance, within a regenerative context.[6] Finally, the hydrogel platform could be used for different applications, for instance as a substrate to accommodate direct bioprinting of an hSE,[11,29] in order to automatize the fabrication procedure.

4. Conclusion

We have developed a 3D platform containing nociceptor-innervated skin of human origin, recapitulating the native manner of innervation, that can be easily observed without sample sectioning. Using this platform, we demonstrated the potential to evaluate the effect of topical compounds on innervating fibers. We believe that this pilot work contributes toward the pursuit

platform. C) Bead object count was performed by analyzing and counting circular objects in the images within a defined threshold. The boxplot shows data points from the minimum to maximum value. D) Neurite degeneration was obtained by dividing this value by the total neurite area. The bar graphs represent the mean + SD. Statistics were performed using one-way ANOVA followed by Tukey's HSD post hoc test, where $***p < 0.001$, $**p < 0.01$, and $*p < 0.05$. One experiment ($n = 4$) was performed.

of biomimetic and functional skin models for improved preliminary *in vitro* research that may enhance predictability of results in following animal and human trials.

5. Experimental Section

Agarose Microwell Platform Fabrication: A 3% (w/v) sterile agarose (Thermo Fisher Scientific) solution was prepared in phosphate buffered saline (PBS). 8 mL of agarose solution was poured onto an in-house fabricated PDMS stamp with the negative template of 1580 microwells with 400 µm diameter. Centrifugation at 3500 rpm was performed to remove air bubbles, followed by chilling for 45 min at 4 °C for agarose solidification. When solid, the agarose blocks were removed, cut to fit in a 12 well-plate, washed with 70% ethanol, then washed twice in PBS solution and left at 4 °C until further use. The day before cell seeding, PBS was replaced with culture media containing Advanced RPMI 1640 supplemented with 1× glutamax (Thermo Fisher Scientific) and kept in the incubator at 37 °C, 5% CO_2 overnight.

iPSCs Culture: Human iPSC line LUMC0031iCTRL08 (provided by the iPSC core facility of Leiden University Medical Center) was cultured on Geltrex coated dishes at a density of 10×10^3 cells cm^{-2} in mTESR1 medium (Stem Cell Technology). Cells were fed every alternate day with completely fresh medium and passaged weekly using Accutase (Stem Cell Technology). Upon splitting, cells were cultured in mTESR1 medium supplement with 10×10^{-6} M of Y-27632 (Tocris) for 24 h and replaced with mTESR1 medium for further maintenance.

iPSCs Differentiation into Nociceptive Neurons and Neurosphere Formation: In order to induce iPSCs differentiation into nociceptors, the protocol published by Chambers et al.[30] was adapted and modified. Nociceptor induction was initiated using single cell suspension of undifferentiated iPSCs detached with accutase, followed by seeding of 200 cells/microwell in mTESR1 medium supplemented with 10 µm of Y-27632 and 0.5% Geltrex (in solution) onto 400 µm agarose microwells. Cell suspension was forced to settle by centrifugation at 1200 rpm for 2 min. Afterward, cells were incubated for 24 h and were given a complete media change with mTESR1 medium. At this time, the cellular spheroid was formed and cell synchronization was initiated by the addition of mTESR1 medium supplemented with 1% dimethyl sulfoxide (DMSO). The cells were maintained for 72 h in the synchronization medium. Post synchronization, cells were given a PBS wash and nociceptor induction was initiated by addition of dual SMAD inhibition media containing Advanced RPMI 1640 supplemented with Glutamax (both Thermo Fisher Scientific), 100×10^{-9} M LDN-193189 (Tocris) and 10×10^{-6} M SB431542 (Tocris). The spheres were maintained for 48 h in the dual SMAD inhibition media. Following this, neural crest commitment was induced via media containing Advanced RPMI 1640 supplemented with Glutamax, 3×10^{-6} M CHIR99021 (Tocris) and 1×10^{-6} M retinoic acid (Tocris). The spheres were maintained in the neural crest induction media for 5 days with media change every alternate day. Following this stage, the spheres were incubated in Notch inhibition media, consisting of Advanced RPMI supplemented with Glutamax, 10×10^{-6} M SU5402 (Tocris) and 10×10^{-6} M DAPT (Tocris), for 48 h.

Finally, the neurospheres, composed of trunk neural crest cells, were collected and seeded on coverslips or scaffolds. In these substrates, cells were cultured in neural maturation medium for at least 5 days to reach the nociceptor phenotype. The neural medium is composed of neurobasal medium, 0.5×10^{-3} M Glutamax, 100 U mL^{-1} penicillin, and 100 µg mL^{-1} streptomycin (all Thermo Fisher Scientific), 100 ng mL^{-1} human NGF, 50 µg mL^{-1} ascorbic acid (all Sigma-Aldrich), 25 ng mL^{-1} human neuregulin-1 type III (NRG-1 SMDF), and N21 supplement (both from R&D systems).

Characterization of iPSCs-Derived Nociceptors Phenotype: To characterize the formation of nociceptor neurons from iPSCs and compare their phenotype with DRG neurons, the neurospheres (at the end stage of differentiation) and DRGs were seeded on 12 mm laminin-coated coverslips (one sphere/DRG per coverslip). Laminin coating was performed the day before cell seeding, with 100 µL of a solution containing 1 µg mL^{-1} laminin-1 (R&D systems) and 2 µg mL^{-1} poly-D-lysine (Sigma Aldrich) in PBS. The neurons were cultured for 7 days in neural medium composed of neurobasal medium, 0.5×10^{-3} M Glutamax, 100 U mL^{-1} penicillin, and 100 µg mL^{-1} streptomycin (all Thermo Fisher Scientific), 100 ng mL^{-1} human NGF, 50 µg mL^{-1} ascorbic acid (both Sigma-Aldrich) and N21 supplement (R&D systems). At day 7 of culture, the cells were fixed and immunostained as described below.

3D Culture of DRGs and iPSCs Neurospheres in a Collagen/Fibrin Matrix: 3D neuron cultures were performed by combining a neuron-seeded scaffold with a collagen/fibrin hydrogel. The scaffold was prepared by punching a 12 mm circular section from a nonwoven polyurethane mesh (6691 LL, Lantor B.V.). These sections were then sterilized by immersion in 70% ethanol for 1 h and transferred to sterile 24-well plates. iPSCs neurospheres were collected from the agarose platforms and seeded on these scaffolds (one neurosphere per scaffold). The samples were cultured in neural medium and left to attach overnight, at 37 °C, 5% CO_2. The same procedure was done for DRG cultures. To isolate DRGs, P7 Brown Norway rats were dissected, previously sacrificed by decapitation (following local and Dutch animal use guidelines). After collection, the DRG was carefully stripped from nerve roots and placed on the scaffold.

The day after, a sterile ice-cold solution of collagen type I (rat tail, Corning, 354249), fibrinogen (human, Enzyme Research Laboratories), thrombin (bovine, Sigma-Aldrich, T4648), NaOH (1N), PBS (10×), and deionized H_2O was prepared, to yield a final concentration of 4 mg mL^{-1} of collagen and 1 mg mL^{-1} of fibrin. 200 µL of this solution was added on top of the cell-seeded scaffold and left to polymerize for 15 min at 37 °C, 5% CO_2. The cells were cultured for 7 days with neural medium, at 37 °C, 5% CO_2.

Human Tissue and Cell Culture: Human foreskin was obtained after routine circumcisions from surgery. All skin samples were obtained in compliance with the "Code for Proper Secondary Use of Human Tissue" as formulated by the Dutch Federation of Medical Scientific Societies (www.federa.org) and approved by the institutional review board of the VU University medical center.

Keratinocytes and fibroblasts were isolated from foreskin and cultured essentially as previously described.[31] Keratinocytes were expanded in keratinocyte medium (KC medium) composed of Dulbecco's modified Eagle's medium (DMEM)/Ham's F12 (Corning) in a 3:1 ratio supplemented with 1% UltroserG (BioSepra SA), 1 µmol L^{-1} hydrocortisone (Sigma-Aldrich), 1 µmol L^{-1} isoproterenol hydrochloride (Sigma-Aldrich), 0.1 µmol L^{-1} insulin (Sigma-Aldrich), 2 ng mL^{-1} human keratinocyte growth factor (Sigma-Aldrich), 100 U mL^{-1} penicillin, and 100 µg mL^{-1} streptomycin (Corning). Fibroblasts were cultured in DMEM with 1% UltroserG and 1% penicillin/streptomycin. For all experiments, keratinocytes were used at passage 2 and fibroblasts at passage 2–3.

Formation of Human Skin Equivalent: hSE was constructed as previously described.[16] Fibroblasts (5×10^5 cells) were embedded in 350 µL of a 4 mg mL^{-1} collagen (rat tail) plus 1 mg mL^{-1} fibrin (human; Enzyme Research Laboratories) solution and this mixture pipetted into 24 mm transwell inserts (0.4 µm pore size; Corning). Hydrogels were cultured for 1–3 days submerged in KC medium. Keratinocytes (5×10^5 cells) were then seeded on top of the hydrogel and cultured submerged for 3–4 days in KC medium. Hereafter, hSE were further cultured at the air–liquid interface for another 10–14 d in skin medium composed of DMEM/Ham's F12 in a 3:1 ratio supplemented with 1% UltroserG, 1 µmol L^{-1} hydrocortisone, 1 µmol L^{-1} isoproterenol hydrochloride, 0.1 µmol L^{-1} insulin, 10 µmol L^{-1} L-carnitine, 0.01 mol L^{-1} L-serine, 50 µg mL^{-1} ascorbic acid (Sigma-Aldrich), 2 ng mL^{-1} human keratinocyte growth factor (Sigma-Aldrich), and 1% penicillin/streptomycin.

Fabrication of a Compartmentalized Collagen/Fibrin Platform: The compartmentalized collagen/fibrin platforms were prepared as follows. Briefly, it was started by fabricating the PDMS mold units, which were made by pouring a PDMS solution (10:1 monomer:curing agent) (Farnell) on custom-made molds and curing for 2 h at 80 °C. These custom-made molds (one to produce the reservoir and the other to produce the patterning unit) were created through milling (monoFAB SRM-20, Roland) of a poly(methyl methacrylate) (PMMA) slab. Afterwards, the PDMS units

were cut from the mold and post-cured/sterilized for 4 h at 160 °C and left in sterile conditions until use. To create the compartmentalized collagen/fibrin platforms, the PDMS units were first assembled as demonstrated in Figure 3, and then pipetted 150 µL of a collagen/fibrin solution (4 mg mL^{-1}/1 mg mL^{-1}) inside the reservoir. After this, a scaffold composed of a sterile 8 mm circular cut of a nonwoven polyurethane mesh (6691 LL, Lantor B.V.) was added on top. The platforms were left to polymerize overnight at 37 °C, 5% CO_2 and inside a petri dish filled with PBS to maintain humidity and prevent gel drying. The following day, these could be detached from the PDMS molds, by carefully picking the scaffold with a fine tip tweezer. The hydrogel platforms were left in neural medium until further use.

Development of an Innervated Skin Model Using the Compartmentalized Collagen/Fibrin Platform: The innervated skin model was constructed by sequential co-culture of iPSCs-derived nociceptor neurosphere with a hSE section, as illustrated in Figure 3. Once differentiated, the neurospheres were picked from the mold and added into the neuron compartment of the collagen/fibrin platforms (previously dried up of medium). Immediately, the platforms were centrifuged at 50 *g* for 1 min, to promote cell settling. After this, 15 µL of the same collagen/fibrin solution was added on top of the neurosphere to seal it. The solution was left to polymerize for 15 min by incubation at 37 °C, 5% CO_2. After this, neural medium was added and the cells were cultured for 7 d in the same conditions, with medium refreshments every other day. At day 7, the hSE cultures (at the mature stage) were retrieved and 3 mm diameter circular sections were made using a sterile biopsy punch. These sections were then carefully placed on the skin compartment of the gel platform, previously filled with 15 µL of collagen/fibrin solution, to promote the hSE immobilization. The gel platforms, containing the neurosphere and hSE section, were transferred to 24-well plate inserts (VWR, BRND782807) and fitted into an adequate 24-well plate (Thermo Fisher Scientific, 15503783). The medium composed of skin/neural medium at 1:1 was added without submerging the hSE sections, leaving them exposed to the air. The cells were cultured in this medium and conditions for additional 21 d, at 37 °C, 5% CO_2.

Capsaicin Patch Testing on Innervated Skin Platform: At day 46 of neurosphere culture (day 21 of skin/neuron co-culture), the capsaicin patch test was performed as illustrated in Figure 5. For this, 3 mm diameter circular cuts of a capsaicin patch (Qutenza) were made using a sterile biopsy punch, and the cuts were placed directly in contact with the stratum corneum of the skin section. The samples were incubated for 1 or 24 h, in neural/skin medium, at 37 °C, 5% CO_2.

Immunostaining: Samples were fixed with 4% paraformaldehyde (PFA) for 25 min at room temperature (RT), rinsed thoroughly with PBS, and left in PBS until further use. Permeabilization and blocking were performed simultaneously with a solution of 1% triton X-100, 5% goat serum, 0.05% Tween20, and 1% bovine serum albumin (BSA) in PBS, for 24 h at 4 °C, under mild agitation. Immediately, samples were incubated for 48 h at 4 °C, under mild agitation, with primary antibody solutions containing 0.1% triton X-100, 5% goat serum, 0.05% Tween20, and 1% BSA in PBS. Following this, the samples were washed with a wash buffer composed of 0.05% Tween20 and 1% BSA in PBS, and left for 24 h at 4 °C, under mild agitation, to remove unbound antibodies. Secondary antibody solutions were prepared in wash buffer and incubated for 48 h at 4 °C, under mild agitation. Following this, the samples were rinsed with PBS, stained with DAPI (0.2 µg mL^{-1}) for 20 min at RT, and left them in PBS until imaging.

The used primary antibodies were the following: anti-βIII tubulin (Sigma-Aldrich, T8578, 1:500), anti-Substance P (Abcam, ab14184, 1:100), anti-CGRP (Abcam, ab22560, 1:500), anti-TRPV-1 (Alomone Labs, ACC-030, 1:100), and anti-involucrin (Abcam, ab181980, 1:100).

Finally, the used secondary antibodies were the following: goat anti-mouse conjugated with Alexa Fluor 488, goat anti-mouse conjugated with Alexa Fluor 568, goat anti-rabbit conjugated with Alexa Fluor 488, and donkey anti-sheep conjugated with Alexa Fluor 488 (all Thermo Fisher Scientific).

Microscopy and Image Analysis: Stereomicroscope images were acquired with a Nikon SMZ25 stereomicroscope. Fluorescent images were acquired with an inverted epifluorescence microscope (Nikon Eclipse Ti-e) or a confocal laser scanning microscope (Leica TCS SP8). 3D image reconstructions were processed with Amira (Thermo Fisher Scientific). All the other images were prepared and analyzed using Fiji software (https://fiji.sc/). To determine the axonal degeneration resultant from the capsaicin exposure experiment, an algorithm that is able to detect associated morphological changes was developed. The method is illustrated in Figure S7 and is based on the analysis of immunostaining images to βIII-tubulin. The original images were first converted to binary and then the analyzed particle function in Fiji was used to segment objects that represent debris of degenerated axons. This function provides both the object counting and total object area. In addition, the total axonal area was measured. Finally, the object area was divided by the total axonal area to determine the normalized degeneration area.

Statistical Analysis: Boxplots are shown as data points from the minimum to maximum value. Bar graphs represent the mean + SD. Statistics were performed using an unpaired *t*-test or a one-way ANOVA followed by Tukey's HSD post hoc test. The asterisks represent: $***p < 0.001$; $**p < 0.01$; $*p < 0.05$ and n.s. means $p > 0.05$. One batch of hSE was used to perform each experiment with four replicates within the experiment.

Supporting Information

Supporting Information is available from the Wiley Online Library or from the author.

Acknowledgements

A.C. contributed with rheology tests done in revision. The authors would like to acknowledge Irit Vahav (Amsterdam UMC) for assisting in skin model construction. The authors would like to thank the Dutch province of Limburg for the project funding. This work was partly supported by the research program VENI 2017 STW- project 15900 financed by the Dutch Research Council (NWO).

Conflict of Interest

The authors declare no conflict of interest.

Data Availability Statement

The data that support the findings of this study are available from the corresponding author upon reasonable request.

Keywords

3D in vitro model, biofabrication, electrospinning, innervation, skin

Received: September 13, 2022
Published online: November 14, 2022

[1] B. Laverdet, A. Danigo, D. Girard, L. Magy, C. Demiot, A. Desmoulière, *Histol. Histopathol.* **2015**, *30*, 875.
[2] E. Emmerson, *J. Invest. Dermatol.* **2016**, *137*, 543.
[3] M. J. Randall, A. Jüngel, M. Rimann, K. Wuertz-Kozak, *Front. Bioeng. Biotechnol.* **2018**, *6*, 154.
[4] P. Anand, K. Bley, *Br. J. Anaesth.* **2011**, *107*, 490.
[5] B. Frias, Merighi, A. Capsaicin, *Molecules* **2016**, *21*, 797.
[6] M. Blais, L. Mottier, M.-A. Germain, S. Bellenfant, S. Cadau, F. Berthod, *Tissue Eng., Part A* **2014**, *20*, 2180.

[7] V. Parfejevs, J. Debbache, O. Shakhova, S. M. Schaefer, M. Glausch, M. Wegner, U. Suter, U. Riekstina, S. Werner, L. Sommer, *Nat. Commun.* **2018**, *9*, 236.
[8] E. Emmerson, *J. Invest. Dermatol.* **2017**, *137*, 543.
[9] H. Miyazaki, Y. Tsunoi, T. Akagi, S. Sato, M. Akashi, D. Saitoh, *Sci. Rep.* **2019**, *9*, 7797.
[10] J. Lee, C. C. Rabbani, H. Gao, M. R. Steinhart, B. M. Woodruff, Z. E. Pflum, A. Kim, S. Heller, Y. Liu, T. Z. Shipchandler, K. R. Koehler, *Nature* **2020**, *582*, 399.
[11] W. L. Ng, J. T. Z. Qi, W. Y. Yeong, M. W. Naing, *Biofabrication* **2018**, *10*, 025005.
[12] C. Pellevoisin, C. Bouez, J. Cotovio, *Skin Tissue Models*, Elsevier, Amsterdam **2018**.
[13] Q. Muller, M.-J. Beaudet, T. De Serres-Bérard, S. Bellenfant, V. Flacher, F. Berthod, *Acta Biomater.* **2018**, *82*, 93.
[14] A. Malheiro, A. Harichandan, J. Bernardi, A. Seijas-Gamardo, G. F. Konings, P. G. A. Volders, A. Romano, C. Mota, P. Wieringa, L. Moroni, *Biofabrication* **2022**, *14*, 014105.
[15] I. Vahav, L. J. Broek, M. Thon, H. N. Monsuur, S. W. Spiekstra, B. Atac, R. J. Scheper, R. Lauster, G. Lindner, U. Marx, S. Gibbs, *J. Tissue Eng. Regener. Med.* **2020**, *14*, 761.
[16] I. J. Kosten, J. K. Buskermolen, S. W. Spiekstra, T. D. De Gruijl, S. Gibbs, *J. Immunol. Res.* **2015**, *13*, 2015.
[17] A. E. Dubin, A. Patapoutian, *J. Clin. Invest.* **2010**, *120*, 3760.
[18] B. Holt, A. Tripathi, J. Morgan, *J. Biomech.* **2008**, *41*, 2689.
[19] S. Gibbs, H. M. Van Den Hoogenband, G. Kirtschig, C. D. Richters, S. W. Spiekstra, M. Breetveld, R. J. Scheper, E. M. De Boer, *Br. J. Dermatol.* **2006**, *155*, 267.
[20] S. Yagihashi, H. Mizukami, K. Sugimoto, *J. Diabetes Invest.* **2011**, *2*, 18.
[21] S. J. Weller, G. D. Baldridge, U. G. Munderloh, H. Noda, J. Simser, T. J. Kurtti, *J. Clin. Microbiol.* **1998**, *36*, 1305.
[22] P. Smith, M. Liu, *Cell Tissue Res.* **2002**, *307*, 281.
[23] D. Roggenkamp, S. Köpnick, F. Stäb, H. Wenck, M. Schmelz, G. Neufang, *J. Invest. Dermatol.* **2013**, *133*, 1620.
[24] A. Chaudhari, K. Vig, D. Baganizi, R. Sahu, S. Dixit, V. Dennis, S. Singh, S. Pillai, *Int. J. Mol. Sci.* **2016**, *17*, 1974.
[25] X. Gu, F. Ding, D. F. Williams, *Biomaterials* **2014**, *35*, 6143.
[26] A. Vela-Romera, V. Carriel, M. A. Martín-Piedra, J. Aneiros-Fernández, F. Campos, J. Chato-Astrain, N. Prados-Olleta, A. Campos, M. Alaminos, I. Garzón, *Histochem. Cell Biol.* **2019**, *151*, 57.
[27] J. F. Peppin, M. Pappagallo, *Ther. Adv. Neurol. Disord.* **2014**, *7*, 22.
[28] C.-T. Chang, B.-Y. Jiang, C.-C. Chen, *Int. J. Mol. Sci.* **2019**, *20*, 1596.
[29] Y. Huyan, Q. Lian, T. Zhao, D. Li, J. He, *Int. J. Bioprint.* **2020**, *6*, 53.
[30] S. M. Chambers, Y. Qi, Y. Mica, G. Lee, X.-J. Zhang, L. Niu, J. Bilsland, L. Cao, E. Stevens, P. Whiting, S.-H. Shi, L. Studer, *Nat. Biotechnol.* **2012**, *30*, 715.
[31] K. Ouwehand, S. W. Spiekstra, T. Waaijman, R. J. Scheper, T. D. De Gruijl, S. Gibbs, *J. Leukocyte Biol.* **2011**, *90*, 1027.